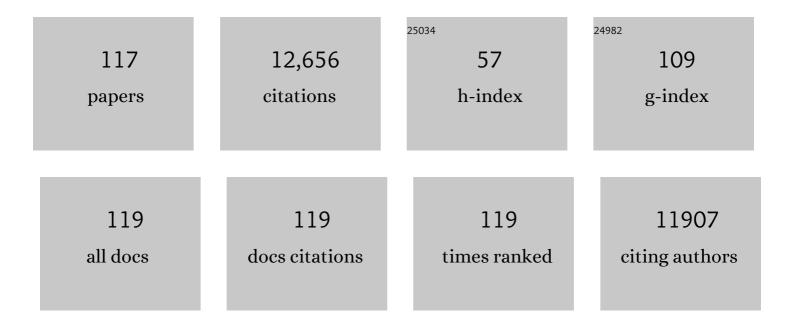
List of Publications by Year in descending order

Source: https://exaly.com/author-pdf/1493824/publications.pdf Version: 2024-02-01



#	Article	IF	CITATIONS
1	Magnetodendrimers allow endosomal magnetic labeling and in vivo tracking of stem cells. Nature Biotechnology, 2001, 19, 1141-1147.	17.5	1,016
2	High-field MRI of brain cortical substructure based on signal phase. Proceedings of the National Academy of Sciences of the United States of America, 2007, 104, 11796-11801.	7.1	610
3	Functional Properties of Brain Areas Associated With Motor Execution and Imagery. Journal of Neurophysiology, 2003, 89, 989-1002.	1.8	592
4	Low frequency BOLD fluctuations during resting wakefulness and light sleep: A simultaneous EEC-fMRI study. Human Brain Mapping, 2008, 29, 671-682.	3.6	521
5	Low-frequency fluctuations in the cardiac rate as a source of variance in the resting-state fMRI BOLD signal. NeuroImage, 2007, 38, 306-320.	4.2	508
6	Magnetic susceptibility mapping of brain tissue in vivo using MRI phase data. Magnetic Resonance in Medicine, 2009, 62, 1510-1522.	3.0	460
7	Water diffusion and acute stroke. Magnetic Resonance in Medicine, 1994, 31, 154-163.	3.0	396
8	Layer-specific variation of iron content in cerebral cortex as a source of MRI contrast. Proceedings of the National Academy of Sciences of the United States of America, 2010, 107, 3834-3839.	7.1	377
9	Large-amplitude, spatially correlated fluctuations in BOLD fMRI signals during extended rest and early sleep stages. Magnetic Resonance Imaging, 2006, 24, 979-992.	1.8	326
10	The relative metabolic demand of inhibition and excitation. Nature, 2000, 406, 995-998.	27.8	296
11	Functional Magnetic Resonance Imaging Brain Mapping in Psychiatry: Methodological Issues Illustrated in a Study of Working Memory in Schizophrenia. Neuropsychopharmacology, 1998, 18, 186-196.	5.4	293
12	Tracking iron in multiple sclerosis: a combined imaging and histopathological study at 7 Tesla. Brain, 2011, 134, 3602-3615.	7.6	282
13	Susceptibility contrast in high field MRI of human brain as a function of tissue iron content. Neurolmage, 2009, 44, 1259-1266.	4.2	266
14	Sensitivity of MRI resonance frequency to the orientation of brain tissue microstructure. Proceedings of the National Academy of Sciences of the United States of America, 2010, 107, 5130-5135.	7.1	238
15	Iron Accumulation in Deep Cortical Layers Accounts for MRI Signal Abnormalities in ALS: Correlating 7 Tesla MRI and Pathology. PLoS ONE, 2012, 7, e35241.	2.5	221
16	Increased iron in the dentate nucleus of patients with Friedreich's ataxia. Annals of Neurology, 1999, 46, 123-125.	5.3	214
17	Sources of functional magnetic resonance imaging signal fluctuations in the human brain at rest: a 7 T study. Magnetic Resonance Imaging, 2009, 27, 1019-1029.	1.8	213
18	The contribution of myelin to magnetic susceptibility-weighted contrasts in high-field MRI of the brain. NeuroImage, 2012, 59, 3967-3975.	4.2	186

#	Article	IF	CITATIONS
19	Micro-compartment specific T2⎠relaxation in the brain. NeuroImage, 2013, 77, 268-278.	4.2	182
20	Design of a SENSE-optimized high-sensitivity MRI receive coil for brain imaging. Magnetic Resonance in Medicine, 2002, 47, 1218-1227.	3.0	180
21	Real-time shimming to compensate for respiration-inducedB0 fluctuations. Magnetic Resonance in Medicine, 2007, 57, 362-368.	3.0	170
22	Modulation of spontaneous fMRI activity in human visual cortex by behavioral state. NeuroImage, 2009, 45, 160-168.	4.2	169
23	Signal-to-noise ratio and parallel imaging performance of a 16-channel receive-only brain coil array at 3.0 Tesla. Magnetic Resonance in Medicine, 2004, 51, 22-26.	3.0	164
24	Pittfalls of MRI measurement of white matter perfusion based on arterial spin labeling. Magnetic Resonance in Medicine, 2008, 59, 788-795.	3.0	159
25	Imaging cortical anatomy by high-resolution MR at 3.0T: Detection of the stripe of Gennari in visual area 17. Magnetic Resonance in Medicine, 2002, 48, 735-738.	3.0	151
26	Application of sensitivity-encoded echo-planar imaging for blood oxygen level-dependent functional brain imaging. Magnetic Resonance in Medicine, 2002, 48, 1011-1020.	3.0	142
27	Restricted and anisotropic displacement of water in healthy cat brain and in stroke studied by NMR diffusion imaging. Magnetic Resonance in Medicine, 1991, 19, 327-332.	3.0	128
28	Extensive heterogeneity in white matter intensity in high-resolution T2*-weighted MRI of the human brain at 7.0 T. NeuroImage, 2006, 32, 1032-1040.	4.2	128
29	Prospective headâ€movement correction for highâ€resolution MRI using an inâ€bore optical tracking system. Magnetic Resonance in Medicine, 2009, 62, 924-934.	3.0	127
30	Functional Mapping of Human Sensorimotor Cortex with 3D BOLD fMRI Correlates Highly with H215O PET rCBF. Journal of Cerebral Blood Flow and Metabolism, 1996, 16, 755-764.	4.3	119
31	T 2 *-based fiber orientation mapping. NeuroImage, 2011, 57, 225-234.	4.2	118
32	A fast gradient-recalled MRI technique with increased sensitivity to dynamic susceptibility effects. Magnetic Resonance in Medicine, 1992, 26, 184-189.	3.0	116
33	Enduring representational plasticity after somatosensory stimulation. NeuroImage, 2005, 27, 872-884.	4.2	112
34	Temporal dynamics of the BOLD fMRI impulse response. NeuroImage, 2005, 24, 667-677.	4.2	110
35	Mapping resting-state functional connectivity using perfusion MRI. NeuroImage, 2008, 40, 1595-1605.	4.2	109
36	Chronic Multiple Sclerosis Lesions: Characterization with High-Field-Strength MR Imaging. Radiology, 2012, 262, 206-215.	7.3	109

#	Article	IF	CITATIONS
37	Invited. On the feasibility of MRI-guided focused ultrasound for local induction of gene expression. Journal of Magnetic Resonance Imaging, 1998, 8, 101-104.	3.4	107
38	Nonexponential <i>T</i> <sub>2</sub> * decay in white matter. Magnetic Resonance in Medicine, 2012, 67, 110-117.	3.0	101
39	The Role of the Medial Wall and Its Anatomical Variations for Bimanual Antiphase and In-Phase Movements. NeuroImage, 2001, 14, 674-684.	4.2	94
40	Metabolic Origin of Bold Signal Fluctuations in the Absence of Stimuli. Journal of Cerebral Blood Flow and Metabolism, 2008, 28, 1377-1387.	4.3	93
41	An adaptive filter for suppression of cardiac and respiratory noise in MRI time series data. NeuroImage, 2006, 33, 1072-1081.	4.2	92
42	Finding thalamic BOLD correlates to posterior alpha EEG. NeuroImage, 2012, 63, 1060-1069.	4.2	92
43	fMRI Applications in Schizophrenia Research. NeuroImage, 1996, 4, S118-S126.	4.2	86
44	Statistical feature extraction for artifact removal from concurrent fMRI-EEG recordings. NeuroImage, 2012, 59, 2073-2087.	4.2	83
45	Improved BOLD detection in the medial temporal region using parallel imaging and voxel volume reduction. NeuroImage, 2006, 29, 1244-1251.	4.2	80
46	Negative BOLD-fMRI Signals in Large Cerebral Veins. Journal of Cerebral Blood Flow and Metabolism, 2011, 31, 401-412.	4.3	80
47	Characterization of a dielectric phantom for highâ€field magnetic resonance imaging applications. Medical Physics, 2014, 41, 102303.	3.0	80
48	Characterization of <i>T</i> <sub>2</sub> * heterogeneity in human brain white matter. Magnetic Resonance in Medicine, 2009, 62, 1652-1657.	3.0	76
49	Fast 3D functional magnetic resonance imaging at 1.5 T with spiral acquisition. Magnetic Resonance in Medicine, 1996, 36, 620-626.	3.0	72
50	Hunting for neuronal currents: absence of rapid MRI signal changes during visual-evoked response. NeuroImage, 2004, 23, 1059-1067.	4.2	71
51	ln vivo quantification of T2⎠anisotropy in white matter fibers in marmoset monkeys. Neurolmage, 2012, 59, 979-985.	4.2	70
52	Scalable multichannel MRI data acquisition system. Magnetic Resonance in Medicine, 2004, 51, 165-171.	3.0	69
53	EPI-BOLD fMRI of human motor cortex at 1.5 T and 3.0 T: Sensitivity dependence on echo time and acquisition bandwidth. Journal of Magnetic Resonance Imaging, 2004, 19, 19-26.	3.4	68
54	A comparison of fast MR scan techniques for cerebral activation studies at 1.5 Tesla. Magnetic Resonance in Medicine, 1998, 39, 61-67.	3.0	63

#	Article	IF	CITATIONS
55	7 Tesla Magnetic Resonance Imaging to Detect Cortical Pathology in Multiple Sclerosis. PLoS ONE, 2014, 9, e108863.	2.5	63
56	Fast Magnetic-Resonance Temperature Imaging. Journal of Magnetic Resonance Series B, 1996, 112, 86-90.	1.6	61
57	Contribution of systemic vascular effects to fMRI activity in white matter. NeuroImage, 2018, 176, 541-549.	4.2	60
58	Fast echo-shifted gradient-recalled MRI: Combining a short repetition time with variable T2* weighting. Magnetic Resonance in Medicine, 1993, 30, 68-75.	3.0	58
59	Monitoring Stem Cell Therapy in Vivo Using Magnetodendrimers as a New Class of Cellular MR Contrast Agents. Academic Radiology, 2002, 9, S332-S335.	2.5	58
60	Reduction of Gradient Acoustic Noise in MRI Using SENSE-EPI. NeuroImage, 2002, 16, 1151-1155.	4.2	55
61	Reproducibility of human 3D fMRI brain maps acquired during a motor task. , 1996, 4, 113-121.		54
62	The Effect of Movement Amplitude on Activation in Functional Magnetic Resonance Imaging Studies. Journal of Cerebral Blood Flow and Metabolism, 1999, 19, 1209-1212.	4.3	54
63	Accelerated parallel imaging for functional imaging of the human brain. NMR in Biomedicine, 2006, 19, 342-351.	2.8	54
64	Hemodynamic nonlinearities affect BOLD fMRI response timing and amplitude. NeuroImage, 2009, 47, 1649-1658.	4.2	52
65	Effects of magnetization transfer on T 1 contrast in human brain white matter. Neurolmage, 2016, 128, 85-95.	4.2	52
66	High-sensitivity single-shot perfusion-weighted fMRI. Magnetic Resonance in Medicine, 2001, 46, 88-94.	3.0	49
67	Single-shot diffusion MRI of human brain on a conventional clinical instrument. Magnetic Resonance in Medicine, 1996, 35, 671-677.	3.0	46
68	Making the most of fMRI at 7ÂT by suppressing spontaneous signal fluctuations. NeuroImage, 2009, 44, 448-454.	4.2	46
69	Gradient-enhanced heteronuclear correlation spectroscopy. Theory and experimental aspects. Journal of Magnetic Resonance, 1992, 100, 282-302.	0.5	44
70	The variability of serial fMRI data. NeuroReport, 2000, 11, 3843-3847.	1.2	44
71	Reduced N-Acetylaspartate in Prefrontal Cortex of Adult Rats with Neonatal Hippocampal Damage. Cerebral Cortex, 2002, 12, 983-990.	2.9	44
72	Investigation of BOLD fMRI resonance frequency shifts and quantitative susceptibility changes at 7 T. Human Brain Mapping, 2014, 35, 2191-2205.	3.6	42

#	Article	IF	CITATIONS
73	Effect of head motion on <scp>MRI B</scp> <sub>0</sub> field distribution. Magnetic Resonance in Medicine, 2018, 80, 2538-2548.	3.0	40
74	The PRESTO technique for fMRI. NeuroImage, 2012, 62, 676-681.	4.2	36
75	Brain myo-inositol level is elevated in Ts65Dn mouse and reduced after lithium treatment. NeuroReport, 2000, 11, 445-448.	1.2	33
76	Technological advances in MRI measurement of brain perfusion. Journal of Magnetic Resonance Imaging, 2005, 22, 751-753.	3.4	32
77	Rapid Three-dimensional MR Imaging Method for Tracking a Bolus of Contrast Agent through the Brain. Radiology, 2000, 216, 603-608.	7.3	29
78	A PRESTO-SENSE sequence with alternating partial-Fourier encoding for rapid susceptibility-weighted 3D MRI time series. Magnetic Resonance in Medicine, 2003, 50, 830-838.	3.0	28
79	Reducing correlated noise in fMRI data. Magnetic Resonance in Medicine, 2008, 59, 939-945.	3.0	28
80	Rapid measurement of brain macromolecular proton fraction with transient saturation transfer MRI. Magnetic Resonance in Medicine, 2017, 77, 2174-2185.	3.0	28
81	A 7T spine array based on electric dipole transmitters. Magnetic Resonance in Medicine, 2015, 74, 1189-1197.	3.0	27
82	Method for functional MRI mapping of nonlinear response. NeuroImage, 2003, 19, 190-199.	4.2	26
83	3D Bolus Tracking with Frequency-Shifted BURST MRI. Journal of Computer Assisted Tomography, 1994, 18, 680-687.	0.9	25
84	Microscopic R2* mapping of reduced brain iron in the Belgrade rat. Annals of Neurology, 2002, 52, 102-105.	5.3	25
85	B0-field dependence of MRI T1 relaxation in human brain. NeuroImage, 2020, 213, 116700.	4.2	25
86	Detection of demyelination in multiple sclerosis by analysis of <mml:math xmlns:mml="http://www.w3.org/1998/Math/MathML" altimg="si1.gif" overflow="scroll"&gt;<mml:msubsup><mml:mrow><mml:mi>T</mml:mi></mml:mrow><mml:mn>2&lt; mathvariant="normal"&gt;*</mml:mn></mml:msubsup><mml:mrow> relaxation at 7 T.</mml:mrow></mml:math 	/mr <b>al<i>s</i>mn</b> >	
87	NeuroImage: Clinical, 2015, 7, 709-714. Resolution and reproducibility of BOLD and perfusion functional MRI at 3.0 Tesla. Magnetic Resonance in Medicine, 2005, 54, 569-576.	3.0	23
88	Cortical lesion hotspots and association of subpial lesions with disability in multiple sclerosis. Multiple Sclerosis Journal, 2022, 28, 1351-1363.	3.0	23
89	Fast volume scanning with frequency-shifted burst MRI. Magnetic Resonance in Medicine, 1994, 32, 429-432.	3.0	22
90	Improved Bloch‧iegert based <i>B<sub>1</sub></i> mapping by reducing offâ€resonance shift. NMR in Biomedicine, 2013, 26, 1070-1078.	2.8	20

#	Article	IF	CITATIONS
91	A torque balance measurement of anisotropy of the magnetic susceptibility in white matter. Magnetic Resonance in Medicine, 2015, 74, 1388-1396.	3.0	20
92	All-night functional magnetic resonance imaging sleep studies. Journal of Neuroscience Methods, 2019, 316, 83-98.	2.5	19
93	White matter intercompartmental water exchange rates determined from detailed modeling of the myelin sheath. Magnetic Resonance in Medicine, 2019, 81, 628-638.	3.0	18
94	Transmit B1-field correction at 7T using actively tuned coupled inner elements. Magnetic Resonance in Medicine, 2011, 66, 901-910.	3.0	16
95	Neuroelectrical Decomposition of Spontaneous Brain Activity Measured with Functional Magnetic Resonance Imaging. Cerebral Cortex, 2014, 24, 3080-3089.	2.9	16
96	Magnetically Labeled Glial Cells as Cellular MR Contrast Agents. Academic Radiology, 2002, 9, S148-S150.	2.5	14
97	Optimizing brain tissue contrast with EPI: A simulated annealing approach. Magnetic Resonance in Medicine, 2005, 54, 373-385.	3.0	14
98	Gradient-enhanced exchange spectroscopy. Journal of Magnetic Resonance, 1992, 97, 419-425.	0.5	13
99	Lesions by tissue specific imaging characterize multiple sclerosis patients with more advanced disease. Multiple Sclerosis Journal, 2011, 17, 1424-1431.	3.0	12
100	Gray and White Matter Brain Volume in Aged Rats Raised onn-3 Fatty Acid Deficient Diets. Nutritional Neuroscience, 2004, 7, 13-20.	3.1	11
101	Effects of large vessels in functional magnetic resonance imaging at 1.5T. International Journal of Imaging Systems and Technology, 1995, 6, 245-252.	4.1	10
102	In vivo evaluation of the effect of stimulus distribution on FIR statistical efficiency in event-related fMRI. Journal of Neuroscience Methods, 2013, 215, 190-195.	2.5	10
103	Tailored excitation using nonlinear <i>B</i> <sub>0</sub> â€shims. Magnetic Resonance in Medicine, 2012, 67, 601-608.	3.0	8
104	Cerebrovascular activity is a major factor in the cerebrospinal fluid flow dynamics. NeuroImage, 2022, 258, 119362.	4.2	8
105	Independent Sources of Spontaneous BOLD Fluctuation Along the Visual Pathway. Brain Topography, 2013, 26, 525-537.	1.8	7
106	Optically controlled switchâ€mode currentâ€source amplifiers for onâ€coil implementation in highâ€field parallel transmission. Magnetic Resonance in Medicine, 2016, 76, 340-349.	3.0	7
107	Spectral characteristics of semisolid protons in human brain white matter at 7 T. Magnetic Resonance in Medicine, 2017, 78, 1950-1958.	3.0	7
108	Impulse response timing differences in BOLD and CBV weighted fMRI. NeuroImage, 2018, 181, 292-300.	4.2	6

#	Article	IF	CITATIONS
109	Receive Coil Arrays and Parallel Imaging for Functional Magnetic Resonance Imaging of the Human Brain. , 2006, 2006, 17-20.		5
110	Timeâ€resolved and spatioâ€temporal analysis of complex cognitive processes and their role in disorders like developmental dyscalculia. International Journal of Imaging Systems and Technology, 2012, 22, 81-96.	4.1	5
111	FMRI based on transitionâ€band balanced SSFP in comparison with EPI on a highâ€performance 0.55 T scanner. Magnetic Resonance in Medicine, 2021, 85, 3196-3210.	3.0	5
112	Optically controlled on oil amplifier with RF monitoring feedback. Magnetic Resonance in Medicine, 2018, 79, 2833-2841.	3.0	3
113	On the potential of sensitivity encoded EPI for BOLD functional brain imaging. NeuroImage, 2001, 13, 7.	4.2	2
114	Sensitivity limitations of high-resolution perfusion-based human fMRI at 7ÂTesla. Magnetic Resonance Imaging, 2021, 84, 135-144.	1.8	2
115	Imaging Techniques for Dynamic Susceptibility Contrast-Enhanced MRI. Medical Radiology, 2005, , 95-108.	0.1	1
116	Background suppressed magnetization transfer MRI. Magnetic Resonance in Medicine, 2020, 83, 883-891.	3.0	1
117	Functional magnetic resonance imaging in normal controls and schizophrenics. Schizophrenia Research, 1995, 15, 103.	2.0	0